Supplementary Information for Hutterer, Glotzer and Mishima "Clustering of centralspindlin is essential for its accumulation to the central spindle and the midbody"

Experimental Procedures

Live observation of HsCYK-4-GFP in dividing HeLa cells. HeLa cells stably expressing HsCYK-4-GFP [1] were cultured on Delta T dishes (Bioptechs) and synchronized by double thymidine block. FRAP experiments were performed on a DeltaVision microscope (Applied Precision) equipped with 488 nm laser for photobleaching. To prevent deformation of the central spindle by the ingressing cleavage furrow, cells were treated with 1 μg/ml cytochalasin D. For TIRF observation, 11 h after the release from the second thymidine arrest, cells were treated with 15 nM cell-permeable dye DRAQ5 (Biostatus) for 5 min to visualize chromosomes. Cells were washed with phenol red-free HEPES-buffered DMEM and overlaid with an agarose slab (~5 mm thickness, 2% (w/v) agarose and 2% (v/v) fetal calf serum in medium). Excess medium was removed by aspiration and the flattened cells were observed by a TIRF microscope system equipped with an UAPO 150xO TIRFM objective, a 1.6X optovar, a 488 nm laser (Olympus), and a temperature controlled stage (Bioptechs). Images were acquired with an iXon+ DU897 EM-CCD camera (Andor) 99 ms exposure, 100 ms cycling time and 2x2 binning.

Preparation of proteins. A HeLa cell line that stably expresses MKLP1 (CHO1/KIF23) tandemly tagged with FLAG and GFP at its N-terminus from its native promoter was generated as reported [2]. To purify the centralspindlin complex,

nocodazole-arrested mitotic cells were lysed with a high salt buffer (200 mM NaCl, 10 mM NaF, 40 mM beta-glycerophosphate, 20 mM HEPES pH7.5, 2 mM $MgCl_2$, 1 mM EGTA, 0.5% Triton X-100) and centralspindlin complex was purified using anti-FLAG antibody beads, eluted with 3xFLAG peptide, bound to anti-GFP antibody beads and eluted with PreScission protease. ZEN-4 deletion constructs were constructed by inserting PCR-amplified fragments into pCBD-TEV-BIO to generate and fusion with an N-terminal chitin-binding domain, a C-terminal linker and a biotin-acceptor sequence (GTGSGGLNDIFEAQKIEWHE) [3]. GFP-tagged derivatives contained GFP between the linker and the biotinylation sequence. Kinesin-1 (K432GFP), contains residues 1-432 of human KIF5B in the pCBD-TEV-EGFP-BIO vector. Recombinant proteins were expressed in *E. coli* BL21 (DE3) codon plus RP (Stratagene). Cells were lysed with high salt buffer (0.25 M NaCl, 10 mM Hepes, 1 mM EGTA, 1 mM $MgCl_2$, 1 mM DTT, 0.1% Triton X-100, 0.1 mM ATP, 1 mM PMSF, 10 μg/ml leupeptin, 10 μg/ml pepstatin, pH7.6) and affinity-purified with chitin beads, followed by elution with tobacco etch virus protease. EGFP-fusion proteins used in Figure 3 were further purified by gel filtration (Superdex 200, GE Healthcare Life Sciences) chromatography (0.25 M KCl, 10 mM Hepes, 1 mM EGTA, 1 mM $MgCl_2$, 1 mM DTT, 25 μM ATP).

Biochemical assays. The solubility assay of centralspindlin in crude HeLa cell lysates was performed as described previously [4]. For in vitro sedimentation experiments, recombinant ZEN-4 proteins purified in the presence of high salt were diluted into to a final protein concentration of ~0.2 mg/ml (~50 μg/ml for ZEN-4 1-775 in Fig 2C) and

NaCl as follows: 150 mM (Figure 2A and B), 83 mM (Figure 2C, 2D and S3A) or 25 mM (Figure S3F). The sample was centrifuged at 14,000 rpm (k-factor ~50) for 30 min. In this condition, particles with a sedimentation coefficient bigger than ~100 S are precipitated. By extrapolation from globular proteins, ovalbumin (43 kDa, 3.6S), gamma globulin (158 kDa, 7.1 S), catalase (232 kDa, 11.3 S) and thyroglobulin (670 kDa, 19.3 S), for which the sedimentation coefficient is proportional to (molecular weight)$^{2/3}$, we estimate that the minimum molecular weight of the particles that can be precipitated by this condition is ~7 MDa. For quantification, gels stained with Coomassie Brilliant Blue were scanned and the intensities of the ZEN-4 bands were analysed with ImageJ (http://rsbweb.nih.gov/ij/). Microtubule bundling assay by sedimentation was performed as described previously [4] except that the reaction buffer contained 50 mM NaCl plus 75 mM KCl and CYK-4 (1-232) and ZEN-4 fragments expressed in *E. coli* were used (final 20 μg/ml, respectively). CYK-4 binding assay by coexpression in *E. coli* was done as described previously without the elution step [5]. CYK-4 binding assay with in vitro translated proteins was done as described previously [4].

Analysis of the motility of GFP-tagged motor proteins along immobilized microtubules. Microscope chambers with Taxol-stabilized microtubules immobilized on the coverglass were prepared as reported [6] except that ultraclean coverglasses (ThermoFisher Scientific, Portsmouth, NH) were treated with Sigmacote (Sigma). GFP-tagged motor proteins were introduced into the assay chamber in buffer containing 1 mg/ml casein, 25 mM KCl, 10 mM PIPES (pH 6.8), 3 mM $MgCl_2$, 1 mM

EGTA, 1 mM ATP, 10 mM DTT, 10 mM glucose, 100 μg/ml glucose oxidase, 100 μg/ml catalase, and10 μM paclitaxel. For the assay at 135 ng/ml, ZEN-4::GFPs were first diluted to 45 μg/ml in the assay buffer, followed by additional 330-fold dilution. For artificial oligomerization by avidin, 5 μg/ml of NeutrAvidin (Molecular Probes) was included in the first dilution step. Images were acquired with an iXon+ DU897 EM-CCD camera (Andor) on a CellR TIRFM total internal reflection fluorescence microscope system equipped with an UAPO 150xO TIRFM objective and a 488 nm laser (Olympus). The standard exposure time was 99 ms (100 ms cycling time). Particles moving along microtubules were detected by combination of automated tracking using the ParticleTracker plugin [7] for ImageJ software (http://rsb.info.nih.gov/ij/) and manual validation. Particles associated with microtubules for longer than 0.5 s were further analysed using custom programs based on GNU Octave (http://www.octave.org). Initial particle intensity was calculated as the maximum moving average of the intensities of five time points. For comparison between different samples, the particle intensities were normalized against the half of the average initial intensity of the particles that showed two step photobleaching, i. e., contained two fluorescently active GFPs. The fluorescence intensity distribution of oligomeric clusters containing n GFPs was simulated by the formula,

$$\sum_{k=1}^{n} \binom{n}{k} p^k (1-p)^{n-k} f(kI_{\mathrm{GFP}}, k\sigma^2)$$

, where p is the fraction of fluorescently active GFPs and $f(x, y)$ is the probability density function for a Gaussian distribution with mean, x, and variance, y. For Figure 3P, $p = 0.5$ and $\sigma = 0.3$ were used based on the measurements for dimeric constructs (Figure S4).

Nematode strains. Nematodes were cultured according to standard procedures[8]. The following strains and alleles were used: MG376 (*zen-4(w35) bli-6(sc16)/unc-44(e1260) lag-1(q385)*), BE16 (*bli-6(sc16)*), MT13172 (*mys-1(n4075) V/nT1[qIs51] (IV;V)*).

Generation of transgenic animals. Genomic *zen-4::gfp* plasmids containing an *unc-119* marker were bombarded into *unc-119 (ed3)* animals [9]. Four independent strains each for wild type (*xaIs2, xaIs4, xaIs5 and xaIs7*) and mutant (*xaIs8, xaIs9, xaIs10, xaIs11*) transgenes ([*zen-4(wt or Δ586-603)::gfp unc-119(+)*]) were isolated, in which the transgenes were stably integrated and expressed the GFP-tagged fusion proteins.

Genetic analysis. MG376 was crossed with MT13172 to obtain the strain QM12 *zen-4(w35)*; *bli-6(sc16)/nT1[qIs51] (IV;V). zen-4::gfp* transgenes were introduced into this background by first generating *{Is[zen-4(wt or Δ586-603)::gfp unc-119]}; nT1[qIs51]* and mating animals with both the transgene and the balancer with QM12, resulting in genotypes *zen-4(w35) bli-6(sc16)/nT1[qIs51] {Is[zen-4(wt or Δ586-603)::gfp unc-119]}.* As *zen-4 (w35)* homozygotes and heterozygotes are expected to segregate in 1:4 among non-aneuploid progenies (*nT1[qIs51* contains a recessive lethal mutation), the rescue efficiency was calculated as (the number of rescued *zen-4* homozygotes) / (the number of heterozygotes) x 4.

Live observation of *C. elegans* embryos. Embryos expressing ZEN-4::GFP were imaged by an ERS Spinning Disc confocal system (Perkin Elmer) with a Plan NEO

FLUAR 100x/1.30 objective lens (Zeiss). Forty optical sections covering 40 μm were obtained every minute. For the GFP images in Figure 4C, eleven optical slices corresponding to the centre of embryos were chosen and averaged. The temperature was maintained at 20 °C using a water-cooling plate.

References for Supplement

1. Wolfe, B.A., Takaki, T., Petronczki, M., and Glotzer, M. (2009). Polo-like kinase 1 directs assembly of the HsCyk-4 RhoGAP/Ect2 RhoGEF complex to initiate cleavage furrow formation. PLoS Biol. *7*, e1000110.

2. Poser, I., Sarov, M., Hutchins, J.R., Hériché, J.K., Toyoda, Y., Pozniakovsky, A., Weigl, D., Nitzsche, A., Hegemann, B., Bird, A.W., Pelletier, L., Kittler, R., Hua, S., Naumann, R., Augsburg, M., Sykora, M.M., Hofemeister, H., Zhang, Y., Nasmyth, K., White, K.P., Dietzel, S., Mechtler, K., Durbin, R., Stewart, A.F., Peters, J.M., Buchholz, F., and Hyman, A.A. (2008). BAC TransgeneOmics: a high-throughput method for exploration of protein function in mammals. Nat Methods *5*, 409-415.

3. Beckett, D., Kovaleva, E., and Schatz, P.J. (1999). A minimal peptide substrate in biotin holoenzyme synthetase-catalyzed biotinylation. Protein Sci *8*, 921-929.

4. Mishima, M., Kaitna, S., and Glotzer, M. (2002). Central spindle assembly and cytokinesis require a kinesin-like protein/RhoGAP complex with microtubule bundling activity. Dev Cell *2*, 41-54.

5. Pavicic-Kaltenbrunner, V., Mishima, M., and Glotzer, M. (2007). Cooperative Assembly of CYK-4/MgcRacGAP and ZEN-4/MKLP1 to Form the Centralspindlin Complex. Mol Biol Cell *18*, 4992-5003.

6. Helenius, J., Brouhard, G., Kalaidzidis, Y., Diez, S., and Howard, J. (2006). The depolymerizing kinesin MCAK uses lattice diffusion to rapidly target microtubule ends. Nature *441*, 115-119.

7. Sbalzarini, I.F., and Koumoutsakos, P. (2005). Feature point tracking and trajectory analysis for video imaging in cell biology. J Struct Biol *151*, 182-195.

8. Brenner, S. (1974). The genetics of Caenorhabditis elegans. Genetics *77*, 71-94.

9. Praitis, V., Casey, E., Collar, D., and Austin, J. (2001). Creation of low-copy integrated transgenic lines in Caenorhabditis elegans. Genetics *157*, 1217-1226.

10. Howard, J., and Hyman, A.A. (1993). Preparation of marked microtubules for the assay of the polarity of microtubule-based motors by fluorescence microscopy. Methods Cell Biol *39*, 105-113.

Supplemental Figure Legends

Figure S1 Images of DRAQ5-stained chromosomes of the cell shown in Figure 1B in metaphase and anaphase overlaid to each other (A) or on the HsCYK-4-GFP image (B and C).

Figure S2 Estimation of the in vivo concentration of ZEN-4. *C. elegans* embryos were lysed with 3 volumes of lysis buffer (300 mM NaCl, 20 mM HEPES, 2 mM $MgCl_2$, 10 mM EDTA, 0.5% Triton X-100, 1 mM DTT, 1 mM PMSF, 10 μg/ml leupeptin and 10 μg/ml pepstatin). The indicated amounts of lysate (12.5 mg/ml protein) and recombinant ZEN-4 protein were run on SDS-PAGE and detected by Western blotting using anti-ZEN-4 antibody. Based on the intensities of the ZEN-4 bands, we estimate that 3 μl of lysate contains 6.25 ng ZEN-4, i. e. the concentration of ZEN-4 in the lysate is ~ 2 μg/ml. This corresponds to a concentration of ZEN-4 in the embryo pellet of ~8 μg/ml. This value underestimates the concentration of ZEN-4 in the cell, due to the space between embryos (we estimate this to be ~30% in volume) and the empty volume due to egg shells (~14% in volume based on actual measurement of ~5% in length). Correcting for this factor we obtain ~14 μg/ml as the concentration of ZEN-4 in the cell. Note that this value still underestimates the concentration of ZEN-4 in the cytoplasm as the volume of membranous organelles was not considered. Alternatively, we calculate that ZEN-4 represents ~0.016% of total protein (~ 2 μg/ml ZEN-4 vs 12.5 mg/ml total protein). If we assume that the protein concentration of the cytoplasm is ~100 mg/ml, the concentration of ZEN-4 is estimated to be ~16 μg/ml.

Figure S3 Biochemical characterization of recombinant ZEN-4 proteins. (**A**) Clustering of shorter ZEN-4 fragments was assayed by solubility at 83 mM salt. (**B**) CYK-4-binding was tested by a pull-down assay. Unlabeled, tagged ZEN-4 fragments were translated in vitro and mixed with in vitro translated ^{35}S-labeled CYK-4 (1-232). ZEN-4 fragments were affinity purified and bound CYK-4 was analysed by SDS-PAGE and autoradiography. (**C**) Oligomeric state of ZEN-4 1-775 Δ586-603 was analyzed by Superdex 200 size exclusion chromatography. The peak volume of elution was plotted against theoretical molecular weight of the monomer. Deviation from the standard curve in a similar manner to wild-type full length ZEN-4 and Z601GFP (panel **E**) indicates that the clustering element (586-603) is dispensable for dimerization of ZEN-4. (**D**) Summary of in vitro properties of ZEN-4 deletion constructs. '+/–' for CYK-4 binding of ZEN-4 1-539 denotes that at higher concentrations, it can bind CYK-4 [5]. (**E**) Oligomeric state of GFP-tagged constructs was examined by molecular mass measurement by a multi-angle light scattering detector (DAWN Heleos, Wyatt Technology) connected to a Superdex 200 size-exclusion column in the presence of 250 mM NaCl. Both proteins are dimers in the presence of high salt. (**F**) SDS-PAGE image of solubility assay, indicating that Z585GFP is defective in higher-order cluster formation.

Figure S4 Interaction of Z601GFP with polarity-marked microtubules. The bright section on each microtubule marks the minus-end [10]. (**A**) Z601GFP showed strong accumulation at the plus-end (arrowheads) at 9 μg/ml. (**B**) The kymographs show that

plus-end directed motility of individual particles became discernible at lower protein concentration (135 ng/ml).

Figure S5 Analysis of fluorescence intensities of GFP-tagged motor proteins. (**A**) Estimation of the fraction of fluorescently active GFP. Due to the complex mechanisms of the fluorescence of GFP including fluorophore maturation, blinking behaviour and the possibility of photobleaching during sample preparation and observation, not all the GFP molecules are fluorescently active during observation. Actually, the distributions of the initial intensities of dimeric proteins, K432GFP and Z585GFP, can be fitted well with two superimposed Gaussian curves around I_1 and I_2 (14.2±1.1 and 25.7±2.2, respectively, for K432GFP, 12.3±1.4 and 23.5±2.8 for Z585GFP), indicating that 48% and 42% of the GFP molecules were fluorescently active, respectively. This interpretation of fluorescence intensity distribution is supported by good agreement between I_2 and the mean of the initial intensities of the particles that showed photobleaching in two-steps ($I_{\text{two-steps}}$) (26.8±1.8 (N = 20) for K432GFP and 20.3±1.0 (N = 35) for Z585GFP). (**B**) The time constant of photobleaching of GFP was measured with bright avidin-induced clusters of Z585GFP that remain associated with microtubules for the duration of filming (10 s) by entrapment at the plus-end of microtubules. Sum of the intensities showed exponential decay by photobleaching. The decay time constant estimated by fitting was 4.5 ± 0.1 s.

Figure S6 Analysis of motility of Z585GFP, Z601GFP and K432GFP. Histograms represent the distributions of association time (**A, D, G, J** & **M**), velocity (**B, E, H, K**

& **N**) and run length (**C, F, I, L** & **O**) of individual particles that were observed associated with a microtubule for longer than 0.5 s. For association time and run length, mean (standard error) values calculated by fitting to an exponential decay are indicated. Bins excluded for fitting are indicated with faint colour. For **A** and **J**, arithmetic mean (standard error) values are also shown. Velocity of each particle was calculated by fitting mean square displacement data with a quadratic curve.

A

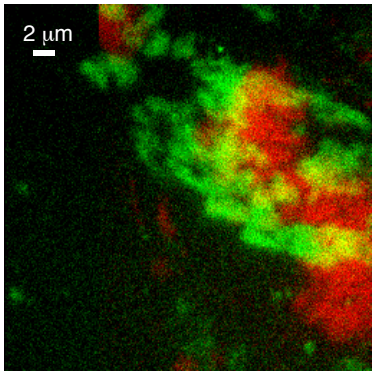

meta DNA
ana DNA

B

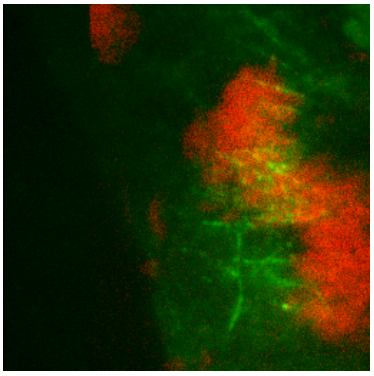

meta DNA
ana HsCYK-4

C

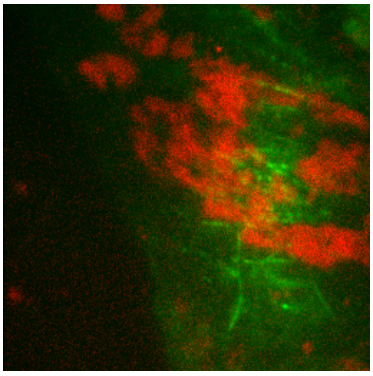

ana DNA
ana HsCYK-4

Hutterer et al. Figure S1

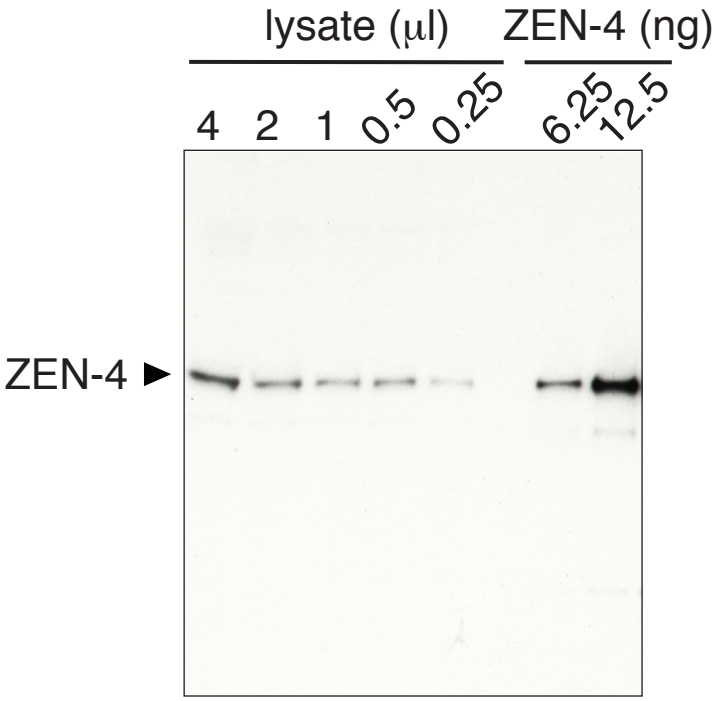

Hutterer et al. Figure S2

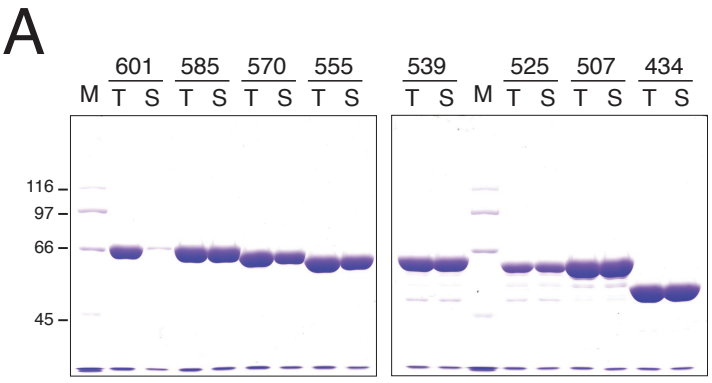

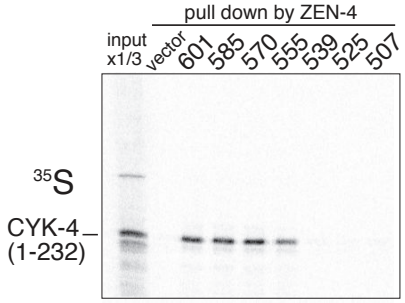

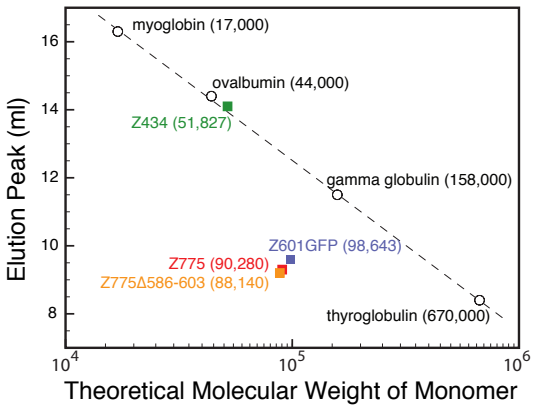

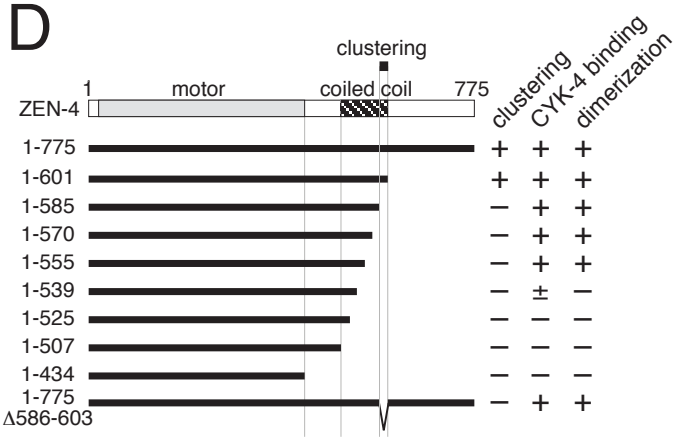

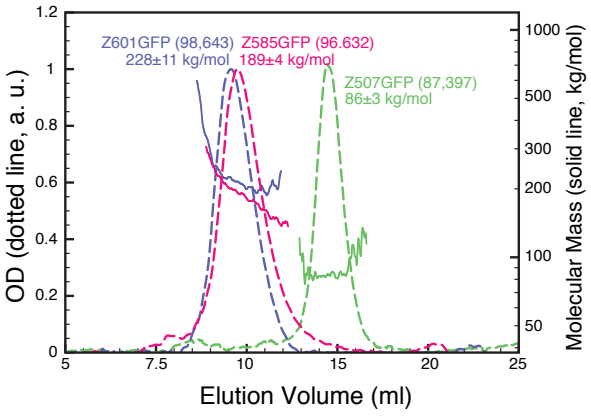

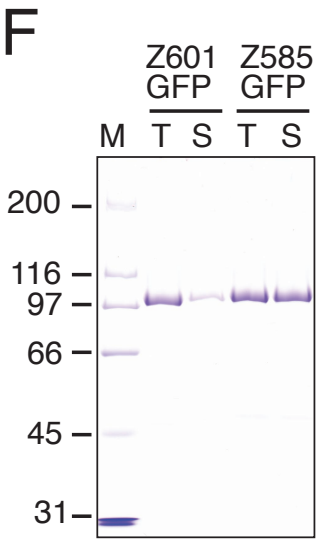

Hutterer et al. Figure S3

A

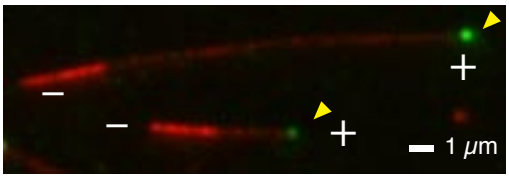

B

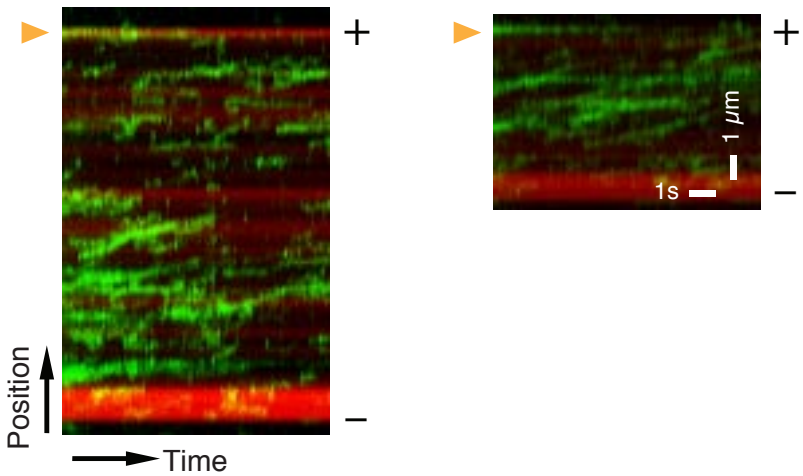

Hutterer et al. Figure S4

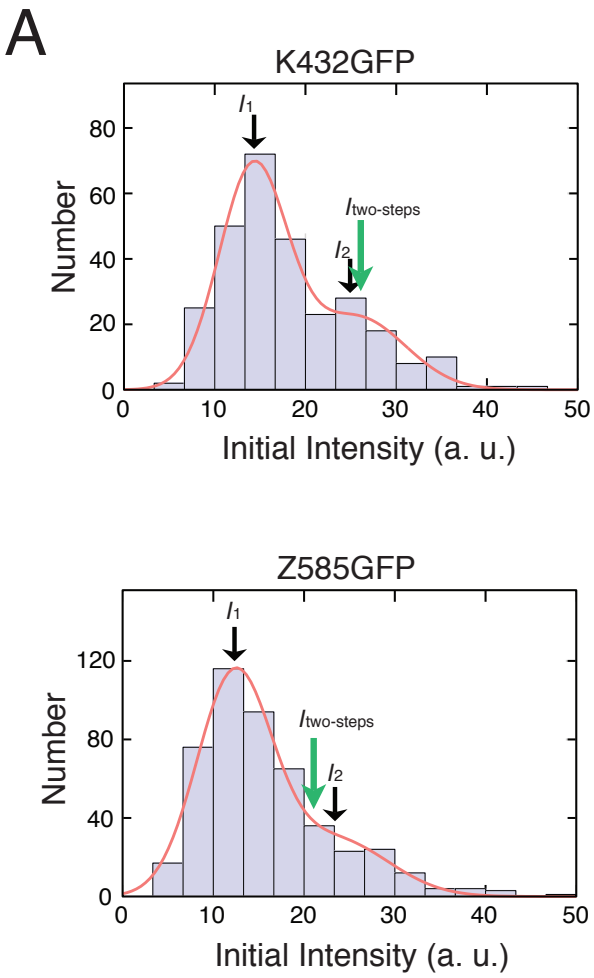

Hutterer et al. Figure S5

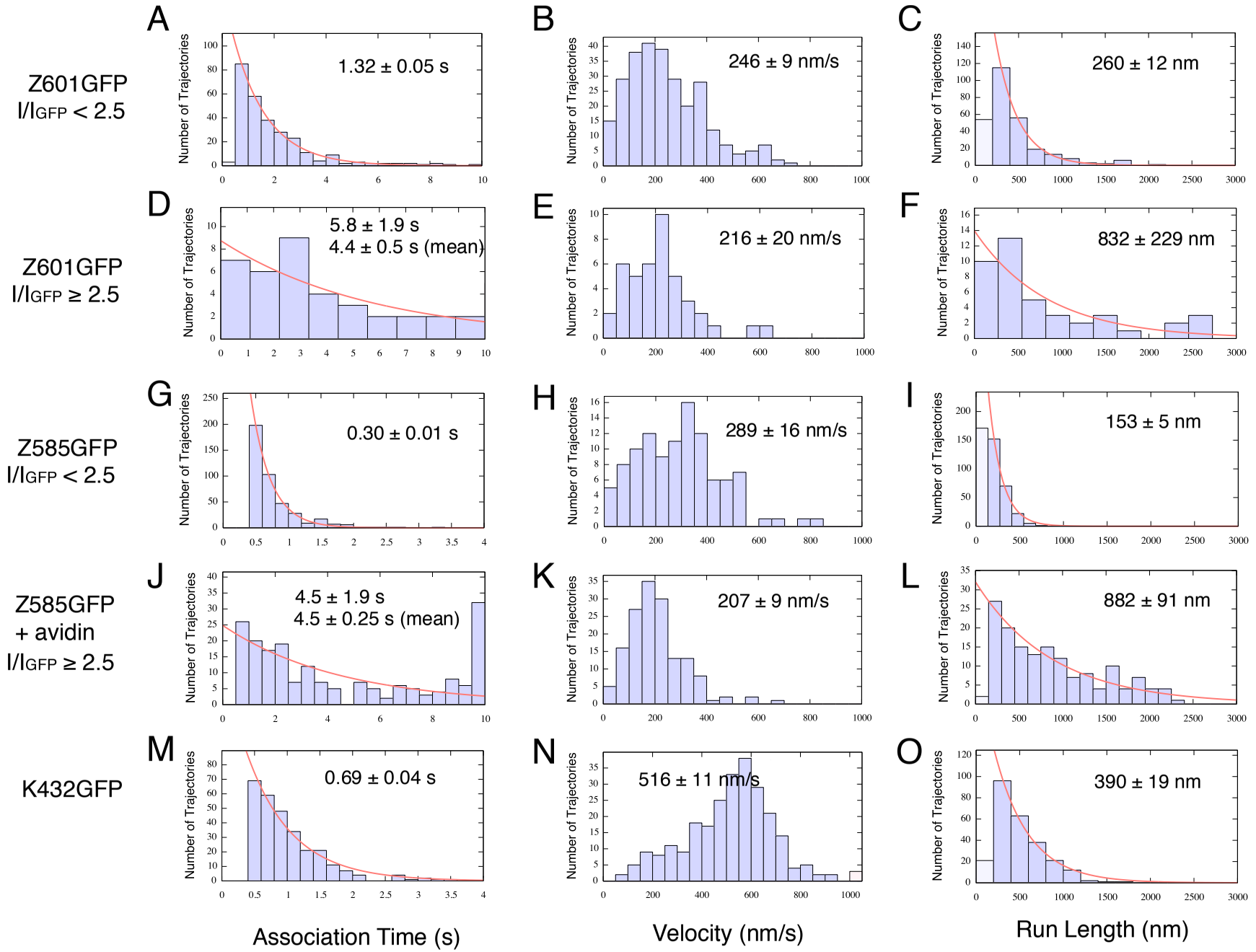

Hutterer et al. Figure S6

Captions for Supplementary Videos

Supplementary Video 1 (hutterer_mov1.mov, QuickTime, 6.2 MB)
Motility of HsCYK-4-GFP clusters in anaphase HeLa cells. The TIRF images of GFP were recorded in continuous mode at 100 ms per frame. Video playback is 2x real-time. The timelapse segments are repeated with color-coded '+' markers to indicate particle 1 to 4 from Figure 1.

Supplementary Video 2 (hutterer_mov2.mov, QuickTime, 4.1 MB)
Movement of Z601GFP (green) along microtubules immobilized on the surface of coverglass (red). The TIRF images of GFP were recorded in continuous mode at 100 ms per frame and overlaid onto one static epifluorescence image of the microtubules. Video playback is 5x real-time.

Supplementary Video 3 (hutterer_mov3.mov, QuickTime, 3.5 MB)
Z585GFP dimer (green) with microtubules immobilized on the surface of coverglass (red). The TIRF images of GFP were recorded in continuous mode at 100 ms per frame and overlaid onto one static epifluorescence image of the microtubules. Video playback is 5x real-time.

Supplementary Video 4 (hutterer_mov4.mov, QuickTime, 3.7 MB)
Movement of Z585GFP oligomerized by avidin (green) along microtubules immobilized on the surface of coverglass (red). The TIRF images of GFP were

recorded in continuous mode at 100 ms per frame and overlaid onto one static epifluorescence image of the microtubules. Video playback is 5x real-time.